Journal of Saudi Chemical Society (2017) **21**, 990–997

King Saud University

Journal of Saudi Chemical Society

www.ksu.edu.sa
www.sciencedirect.com

ORIGINAL ARTICLE

Photo-assisted electrochemical oxidation of the urea onto TiO_2-nanotubes modified by hematite

Waleed M. Omymen [a], Jelena R. Rogan [a], Branimir Z. Jugović [b], Milica M. Gvozdenović [a], Branimir N. Grgur [a,*]

[a] *Faculty of Technology and Metallurgy, University of Belgrade, Karnegijeva 4, 11020 Belgrade, Serbia*
[b] *Institute of Technical Sciences of the Serbian Academy of Sciences and Arts, Knez Mihailova 35/IV, 11000 Belgrade, Serbia*

Received 28 April 2017; revised 24 May 2017; accepted 30 May 2017
Available online 7 June 2017

KEYWORDS

Photoelectrochemical cell;
Water electrolysis;
Fuel cell;
SILAR

Abstract The electrochemical oxidation of the urea in near neutral pH is investigated on platinum electrode. It is shown that oxidation reaction is practically inhibited up to the potentials of ~0.9 V. The same reaction is investigated onto electrochemically obtained titanium dioxide nanotubes modified by hematite using facile, low-cost successive ion layer adsorption and reaction (SILAR) method. It is shown that such system possesses electrocatalytic activity at very low potentials, and activity can be further improved by the illumination of the electrode in the photo-assisted reaction. The possible application of the photoactive anode is considered in the application of urea based water electrolysis and urea based fuel cell.

1. Introduction

The production of electricity or hydrogen from the waste waters or residues of different industrial processes, is today of enormous interest due to environmental issues and needs for alternative energy sources [1]. Urea, also known as carbamide, was considered as an ideal energy carrier [2]. The yearly production of urea for the manufacture of the fertilizers and other chemicals, exceeds hundred millions of tons worldwide [2]. Also, urea is a main component of the human or animal urine, in the concentration range from 0.15 M to 0.4 M, which annual production exceeds many times than market demand, of 0.5 Mt per day [2,3]. Under certain conditions urea can decompose to nitrate or nitrite, which is a high environmental risk due to possible contaminations of the ground water [4,5]. Thus, the waste waters containing urea should be purified using different removal processes [5].

In principle, there are two methods for the use of urea as energy carriers, hydrogen production via electrolysis of water containing urea [3,6] and as a fuel in the fuel cells [7–9].

Theoretically, during the electrolysis of water containing urea, the following reactions occurred:at the cathode:

$$2H_2O + 2e \leftrightharpoons H_2 + 2OH^- (E_r^o = -0.84V) \quad (1)$$

* Corresponding author at: Faculty of Technology and Metallurgy, University of Belgrade, Department of Physical Chemistry and Electrochemistry, Karnegijeva 4, 11020 Belgrade, Serbia. Fax: +381 113303681.
E-mail address: BNGrgur@tmf.bg.ac.rs (B.N. Grgur).
Peer review under responsibility of King Saud University.

ELSEVIER Production and hosting by Elsevier

http://dx.doi.org/10.1016/j.jscs.2017.05.010

and at the anode [3]:

$$CO(NH_2)_2 + 6OH^- \leftrightharpoons N_2 + CO_2 + 5H_2O + 6e \ (E_r^o = -0.46V) \quad (2)$$

Hence, the theoretical decomposition voltage for such cell under standard conditions is as low as 0.38 V. On the other hand, in the urea based fuel cell the following reaction occurred:at the anode:

$$CO(NH_2)_2 + 6OH^- \leftrightharpoons N_2 + CO_2 + 5H_2O + 6e \ (E_r^o = -0.46V) \quad (3)$$

and at the cathode:

$$O_2 + 2H_2O + 4e \leftrightharpoons 4OH^- \ (E_r^o = 0.401V) \quad (4)$$

with the theoretical open circuit voltage under standard conditions of 0.86 V. Because the urea is a very strong catalytic poison for the platinum as the most common catalysts [10], such reactions are technically possible only in the highly alkaline media to prevent intense corrosion, of for example nickel–cobalt based catalyst [9]. Also, the one product of the urea degradation is carbon dioxide which react with used hydroxide electrolyte lowering the efficiency of the processes and pH.

Consequently, different approaches should be considered for the use of wastewater containing urea as energy carriers, with typical pH near neutral, for example: in microbial fuel cells [11], or in different photoelectrochemical cells [1,12–14]. In the photoelectrochemical cell as a most common photoanode the titanium dioxide nanotube is typically used [15–18]. Unfortunately, the band gap of titanium dioxide is ~3.2 eV permitting the absorption of only in the UV light region, which presents a small fraction of ~5% of total Sun irradiance. To improve absorption in a visible range of the Sun spectra, many different surface modifications of TiO_2 were examined [19–21]. Among others, iron oxide, specifically hematite, α-Fe_2O_3, is the topic of intense investigations [15,16,22–26].

In our previous paper [27] it was shown that applying the simple procedure of titanium dioxide nanotube modification by hematite using SILAR (successive ion layer adsorption and reaction) method could improve photoactivity of TiO_2 in the near neutral solutions. So, the aims of this paper are to investigate the possibility of the urea oxidation using such electrode system, and to examine the possible characteristics of the urea contained water electrolysis and photo fuel cell.

2. Experimental

TiO_2 in the form of nanotube is prepared as already reported [27,28] by anodization of the pure Ti foil (Alfa Aesar) 2 cm × 1 cm, 0.127 mm thick in a solution of 1 M H_3PO_4 with the addition of 0.3 wt.% hydrofluoric acid (p.a. Merck). Briefly summarizing, anodization is performed in a plastic cell with a volume of 100 cm^3, initially increasing the voltage from 0 to 20 V during 20 s, and then oxidizing substrate for 1 h at 20 V, using DC Power Supply HY3003 (Mastech, Germany). For the surface modification of TiO_2 the SILAR procedure is used, starting from methanol solution of 0.05 M $Fe(NO_3)_3 \times 9H_2O$ as a source of iron species, and using a 3.5 wt.% of HClO (Centrohem, Serbia) as a reaction solution. The one SILAR cycle consisted of dipping the TiO_2 for 30 s in iron nitrate solution and drying in hot air, followed by immersion in HClO for 60 s. Among SILAR cycle electrode is rising with pure methanol. The procedure is repeated five times with last immersion in HOCl for 15 min. In order to characterize the iron oxide by XRD, the 20 cm^3 of 0.4 M $Fe(NO_3)_3 \times 9H_2O$ of methanol solution is gradually added, drop by drop, to 200 cm^3 of HOCl, and after 15 min filtrated using Büchner funnel. A part of the as prepared sample is further thermally treated at 450 °C to increase crystallinity in an electric furnace.

Energy Dispersive Spectrometer (EDS) Isis 3.2, with a SiLi X-ray detector (Oxford Instruments, UK), is used for electrodes characterization, while SEM images are obtained using the field emission SEM, MIRA3 TESCAN at 10 kV. For the XRD analysis of the as prepared bulk iron oxide, Ital Structure APD2000 X-ray diffractometer in a Bragg–Brentano geometry using CuKα radiation (λ = 1.5418 Å) and step-scan mode with range of 2θ = 20–80°, is used.

The 100 cm^3 rectangular shaped Plexiglas box, from one side equipped with a quartz disk with a diameter of 3 cm is used as photoelectrochemical cell (PEC). Saturated calomel electrode served as a reference, and a Pt plate of 1 cm^2 as a counter (or working) electrode. All experiments are performed in 0.1 M Na_2SO_4 buffered to pH = 9.2 with 0.05 M $Na_2B_4O_7 \times 10H_2O$ (borax), and with a urea concentration in the range of 5–30 g dm^{-3}. To simulate voltage during electrolysis of water contained urea, stainless steel cathode (A = 1 cm^2) is used, while for the fuel cell simulation, polarization curve of the oxygen reduction from the air at Pt cathode (A = 1 cm^2) is used.

As a light source polychromatic 300 W Osram Ultra-Vitalux lamp with sun-like spectral distribution among 280–780 nm, and in the infra-red region is used. The integral light intensity of 80 mW cm^{-2} is estimated using the Amaprobe SOLAR-100 Meter. The electrochemical experiments are carried out using a Gamry PC3 potentiostat.

3. Results and discussion

In Fig. 1 the SEM images of as synthesized titanium dioxide and iron oxide modified electrode are shown. Fig. 1a reveals that anodization of titanium in a phosphoric acid solution with addition of fluoride leads to the formation of the nanotubular structures (NTs) with the estimated average diameter of tube in the range of 80 to 100 nm. Fig. 1b shows SEM images of modified TiO_2 with iron oxides. Iron oxide forms irregular globular deposits onto surfaces, and also covers the TiO_2 nanotubes.

The EDX spectra of the anodized Ti foil, shown in Fig. 2a, reveal that the atomic Ti to O ratio was 36.6: 63.6 corresponding to the pure TiO_2 phase. The EDS spectra of the TiO_2 modified with iron oxide had the following elemental composition: Ti-39.68 wt.% (19.96 at.%); O-50.28 wt.% (75.71 at.%) and Fe-10.04 wt.% (4.33 at.%). Hence it can be concluded by comparing data with pure TiO_2 EDX spectra, that atomic iron to oxygen ratio is approximately 1:7, corresponding to hydrous iron oxide, ferrihydrite [29,30].

Fig. 3b shows the XRD diffraction pattern of the as synthesized iron oxide, and after annealing treatment at the 450 °C for one hour. The XRD spectra of as synthesized sample (spectra a) correspond to poorly crystalline, almost amorphous form [29,30]. Comparing the XRD pattern with standard cards of: goethite α-FeO(OH) (ICSD 28247), hematite α-Fe_2O_3 (ICSD 161294) and lepidocrocite γ-FeO(OH) (ICSD 247035),

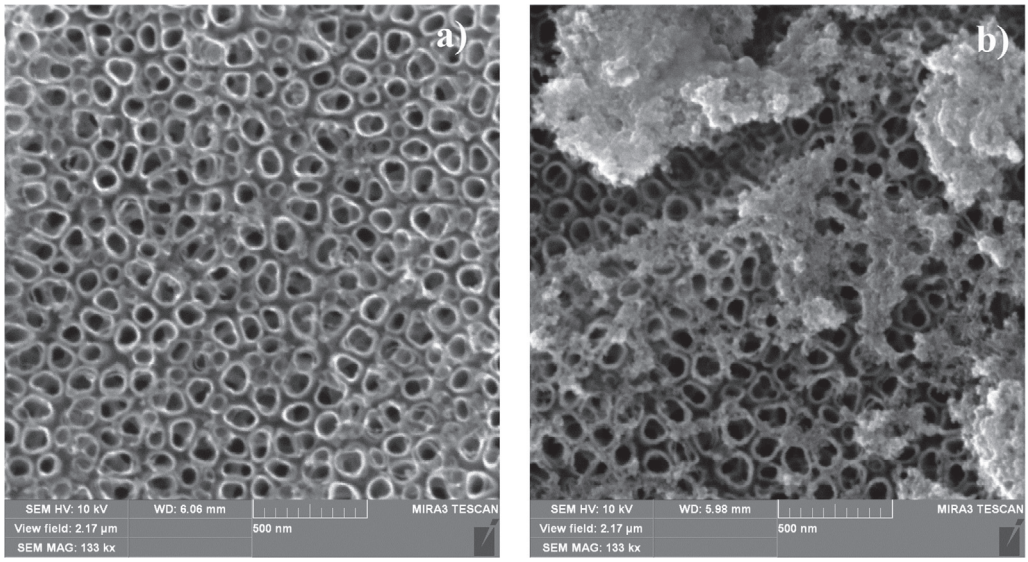

Figure 1 The SEM images of (a) TiO_2; (b) TiO_2 with SILAR deposited iron oxide.

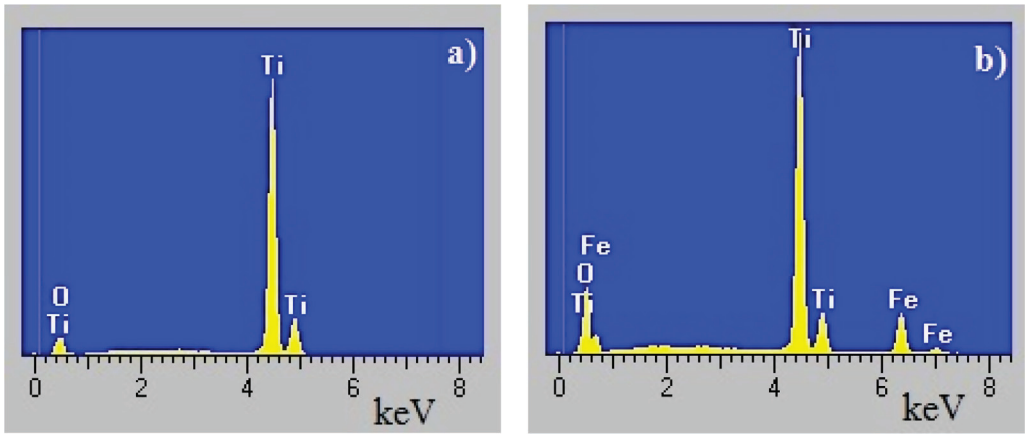

Figure 2 The EDX spectra of (a) TiO_2; (b) TiO_2 with SILAR deposited iron oxide.

it might be carefully concluded that the product is a mixture of α(γ)-FeO(OH) and α-Fe_2O_3. After annealing treatment in order to increase crystallinity (spectra b), and keeping in mind that annealing treatment does not disturb the original phase structure [29], few well defined XRD peaks appear. Using the program PowderCell [31], it is determined that sample contained ~99 wt.% of α-Fe_2O_3 phase. Using the Scherrer formula the mean crystallite size of α-Fe_2O_3 of 32.9 nm is valued. It should be mentioned that strong sample fluorescence is also detected. It is well known that fluorescence greatly contributes to the high intensity of the background of the diffractogram.

3.1. Urea oxidation

3.1.1. Urea oxidation on platinum

In order to investigate the electrochemical urea oxidation, the reaction is first investigated on platinum electrode, and the results are shown in Fig. 4. Without urea in solution, no activity is observed below potential of ~0.8 V (SCE). Above that potential, the oxygen evolution reaction occurred:

$$4OH^- \rightarrow O_2 + 2H_2O + 4e \; E_r = 0.93V \; (SCE) \quad (5)$$

In the presence of 5 g dm^{-3} urea in solution the oxidation starts at low potentials of −0.05 V (SCE). The oxidation occurred up to the potential of 0.15 V (SCE) reaching the maximum current density of 65 μA cm^{-2}, followed by decreased activity at higher potentials. Some additional small activity is observed in the potential range of 0.4 V to 0.75 V. Above 0.9 V the activity is practically identical to platinum without urea in solution. The observed activity at low potentials can be associated with transition phenomena, because under steady state conditions activity rapidly decreases over time, as shown in inset of Fig. 4. By increasing the concentration of the urea to 15 g dm^{-3} the activity decreases for three times, and in solution contained 30 g dm^{-3} of the urea, the activity is insignificant, below potentials of ~0.9 V (SCE).

Using the *in situ* FTIR spectroscopy, Bezerra et al. [10], investigated the adsorption and oxidation of the urea on platinum in different pH of the electrolytes. They found that surface urea adsorbates and the reaction products are dependent on pH of the solutions. At low pH values, *e.g.* in 0.1 M $HClO_4$, the main detected oxidation product is CO_2, while adsorption

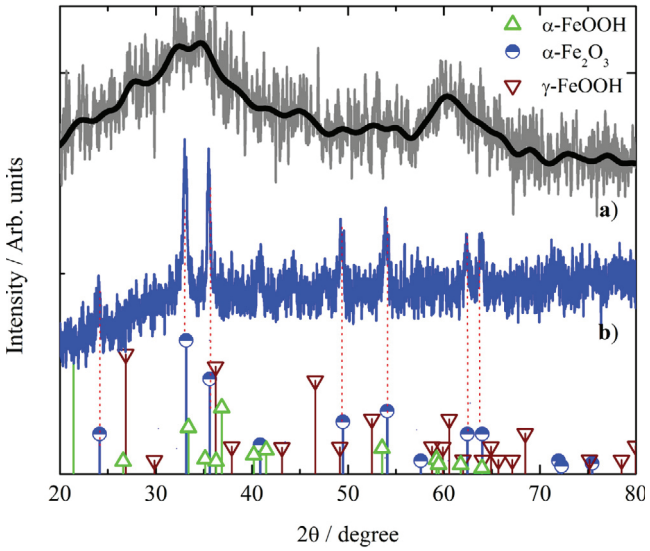

Figure 3 The XRD pattern (a) of as prepared bulk iron oxide and (b) after annealing treatment for 1 h at 450 °C.

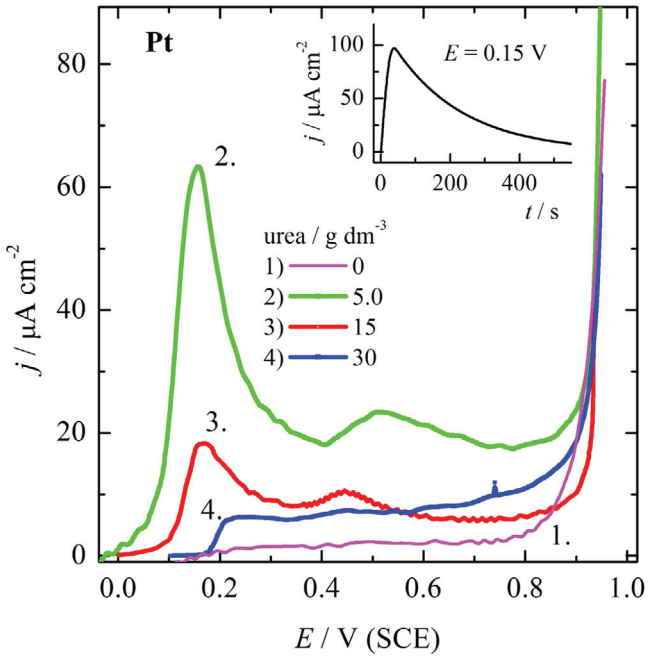

Figure 4 Linear anodic polarization curves (v = 1 mV s^{-1}) of the urea oxidation, in the concentration range from 0 to 30 g dm^{-3}, onto platinum electrode (A = 1 cm^2) at room temperature in the electrolyte containing 0.1 M Na_2SO_4 buffered with 0.05 M borax to pH = 9.2. Inset: potentiostatic pulse at 0.15 V in electrolyte containing 5 g dm^{-3} urea.

of the urea occurred through nitrogen atoms with loss of two hydrogen atoms, followed by the formation of CO due to hydrolysis. In the neutral solutions, *e.g.* 0.1 M KF, the urea adsorption in the double layer proceed with the formation of CNO^- and $[N_2O_2]^{2-}$, and at higher potentials the main detected oxidation products are NO_2 and NO_3^-. In the alkaline solutions, *e.g.* 0.1 M KOH, the urea is adsorbed depending on the potentials via NH_2 group at low potentials and via oxygen atoms at higher potentials. The oxidation products were not reported or proposed.

Thus, based on these results it could be suggested that oxidation of the urea onto platinum occurred via the surface heterogeneous Langmuir–Hinshelwood kinetics [32]. Namely, the reaction involved chemical reaction between adsorbed species onto the surface can be given by the following reaction scheme:

$$Pt + OH^- \rightarrow Pt - (OH)_{ads} + e \quad (6)$$

$$Pt + CH_4N_2O \rightarrow Pt - (CH_4N_2O)_{ads} \quad (7)$$

$$Pt - (OH)_{ads} + Pt - (CH_4N_2O)_{ads} \rightarrow \text{products} \quad (8)$$

Assuming that the rate determining is step given by Eq. (8), the rate of the reaction can be given as:

$$r = k\theta(OH)\theta(CH_4N_2O) \quad (10)$$

where k is the apparent rate constants, and θ surface coverage of the reacting species. It is obvious that the reaction occurred as competitive surface adsorption, for which the maximum rate is under conditions that $\theta(OH) = \theta(CH_4N_2O) = 0.5$. By increasing the $\theta(CH_4N_2O)$, the reaction rate decreases and practically stops when $\theta(CH_4N_2O) \rightarrow 1$. So, increasing the concentration of the urea in solution the rate of the adsorption reaction step, Eq. (7), increased and the rate of the overall reaction decreased.

3.1.2. The photo-electrooxidation of the urea onto TiO_2 modified by hematite

In Fig. 5 the photo-pulsed polarization curves for pure TiO_2-NTs and hematite modified electrode in the supporting electrolyte, are shown. From the inset in Fig. 5, because both electrodes show decrease of the open circuit potentials in negative direction after illumination, it can be concluded that electrodes behave as *n*-type semiconductor.

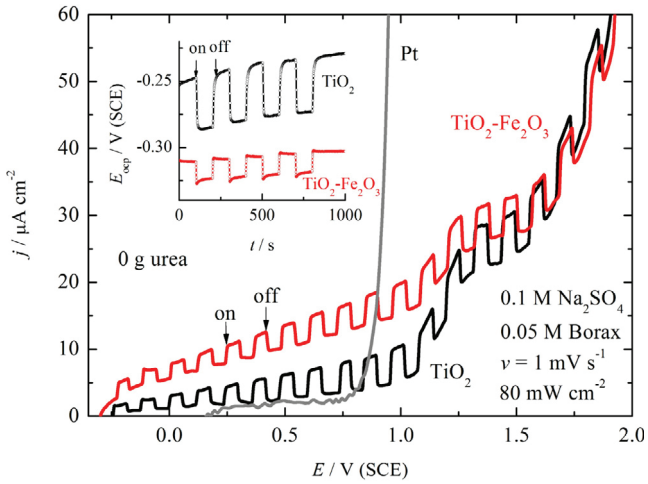

Figure 5 Photo-pulsed (light on–off) polarization curves (v = 1 mV s^{-1}) of TiO_2-NT and hematite modified electrode (A = 2 cm^2) in the supporting electrolyte (0.1 M Na_2SO_4 buffered with 0.05 M borax to pH = 9.2). Inset: The dependence of the open circuit potentials over time under dark and light conditions.

From Fig. 5, it can be seen that both electrodes show photo activity in the anodic direction, from the open circuit potentials. TiO_2-NTs show characteristic photo-response of a thermally untreated sample [15,33–35]. The TiO_2 nanotubes prepared according to the described procedure are amorphous in nature, but after further annealing treatment (under oxidizing conditions in air or O_2), they are transformed to anatase or rutile, which can significantly improve their photo-electrochemical activity [15]. The dark current is higher on the modified electrode, and can be connected with the oxidation of OH^- ions to the hydrogen peroxide ions, according to the previously reported electrochemical route [27]:

$$S + OH^- = S - (OH)_{ads} + e \quad (11)$$

$$S - OH_{ads} + OH^- = S - (H_2O_2)_{ads} + e \quad (12)$$

$$S - (H_2O_2)_{ads} + OH^- = S + HO_2^- + H_2O \quad (13)$$

Under illumination the photocurrent is of the same magnitude as for pure TiO_2-NTs, and reaction can be given as [27]:

$$Fe_2O_3 - S + h\nu \rightarrow Fe_2O_3 - S^* + Fe_2O_3 - CB(e) \quad (14)$$

$$Fe_2O_3 - S^* + OH^- \rightarrow Fe_2O_3 - S - OH_{ads} \quad (15)$$

$$Fe_2O_3 - S^* + Fe_2O_3 - S - OH_{ads} + OH^- \rightarrow Fe_2O_3 - S + Fe_2O_3 - S - (H_2O_2)_{ads} \quad (16)$$

$$Fe_2O_3 - S - (H_2O_2)_{ads} + OH^- \rightarrow HO_2^- + H_2O + Fe_2O_3 - S \quad (17)$$

where S represents the active surface centers (species, $=Fe^{III}—O^-$), S^* iron oxide oxidized surface states (species, $=Fe^{IV}=O$) in which holes are trapped, and CB is conducting band of hematite.

Increased electrochemical and photoelectrochemical activity of TiO_2-NT-hematite modified electrode is explained in more details in reference [27]. Briefly summarizing, on the nanometric interphase edges between TiO_2 and Fe_2O_3, or eventually on the TiO_2 nanotubes covered with a thin nanometric Fe_2O_3 film, Fig. 1b, charge carriers could be efficiently separated. Possibly, the charge is accumulated on Fe_2O_3, because it can benefit from absorption of both visible and UV light, due to smaller band gap of ~2.2 to 2.6 eV than TiO_2 of ~3.2 eV, producing hole-electron pairs. Holes from Fe_2O_3 valence band could be trapped in the surface state, leading to a prolonged lifetime and better oxidation ability. Trapped holes in the surface state, as an electron acceptors, may oxidize OH^- to different products depending on potentials: at low potentials to hydrogen peroxide ions, and at much higher potentials to oxygen. The formed electrons from Fe_2O_3 conducting band can be relocated to TiO_2 conducting band, and further to the external circuit and cathode. The contribution of TiO_2 in the light absorption could be neglected, and should serve as a sink of the electrons as in dye-sensitized solar cells [27].

Fig. 6 shows photo-pulsed polarization curves of TiO_2-NT-hematite modified electrode in the urea contained electrolyte. It can be seen that with increasing the urea concentration both dark and light current increase as well. From the inset of Fig. 6 which shows the comparison of the pulsed and continuous light on or off polarization curves, one can see that the same activity is obtained, consequently the photooxidation should not be connected with some transition phenomena during the switching light on or off. Under constant potential, reaction order based on the urea concentration is determined to be ~0.4 for both light and dark conditions (results are not shown).

In Fig. 7 the polarization curves of TiO_2-NT-hematite modified electrode in the urea contained electrolyte with different concentrations, under constant light on or off conditions are shown. From the figure it can be seen that modified electrode possesses better activity for the urea oxidation than pure TiO_2-NT electrode and Pt electrode at potentials negative than

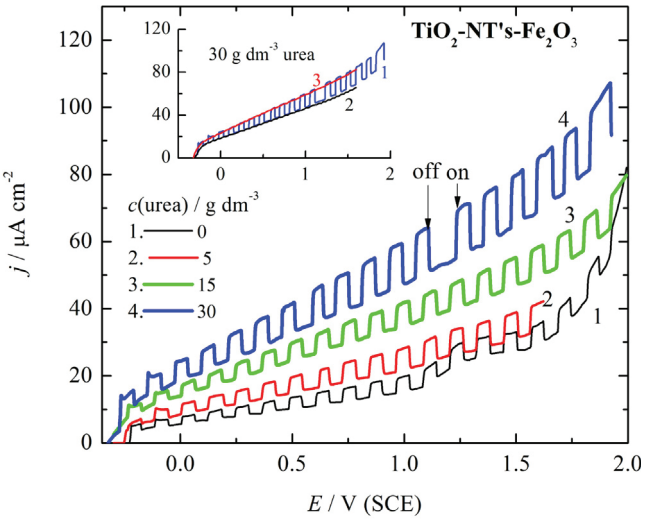

Figure 6 Photo-pulsed (light on–off) polarization curves (v = 1 mV s^{-1}) of TiO_2-NT-hematite modified electrode (A = 2 cm^2) in the urea (concentrations marked in the figure) containing 0.1 M Na_2SO_4 buffered with 0.05 M borax to pH = 9.2 electrolyte. Inset: The comparison of the pulsed (1) and continuous polarization curves with light off (2) or on (3).

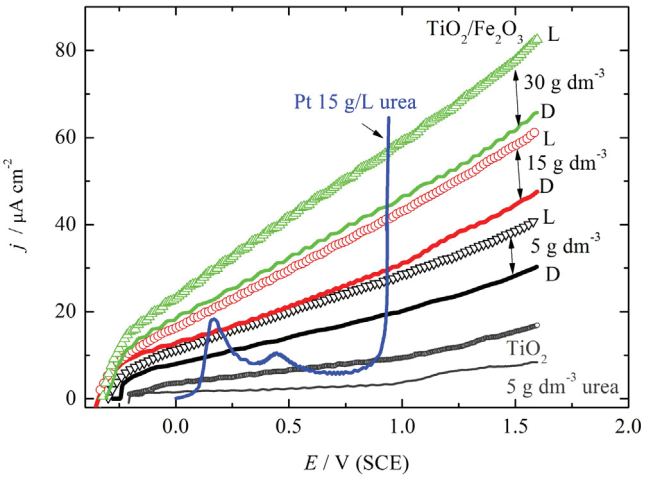

Figure 7 The polarization curves (v = 1 mV s^{-1}) under constant light on (L) or off (D) conditions of TiO_2-NT-hematite modified electrode (A = 2 cm^2) in the urea (concentrations marked in the figure) contained 0.1 M Na_2SO_4 buffered with 0.05 M borax to pH = 9.2 electrolyte, in comparison with pure Pt (A = 1 cm^2) and pure TiO_2-NTs (A = 2 cm^2).

0.9 V, which are shown for comparison. The current density under dark conditions at constant potential increased with increased urea concentration, and additionally for ~30% under light conditions. Hereafter, the electrooxidation of the urea on TiO_2-NT-hematite modified electrode can be considered as a photo-assisted electrochemical reaction.

In accordance with the above shown mechanism, Eqs. (14)–(17), for the overall reaction the photo-activity of the modified electrode could be described with the following equation:

$$Fe_2O_3 - S^* + 3OH^- \rightarrow HO_2^- + H_2O + Fe_2O_3 - S + e \qquad (18)$$

and it could be proposed that urea photo-assisted oxidation, proceeded by the chemical oxidation with adsorbed hydrogen peroxide or with hydrogen peroxide ions near the electrode surface:

$$HO_2^- + CH_4N_2O \rightarrow \text{products} \qquad (19)$$

For the purpose of this work the nature of the products was not investigated.

To test the initial stability, the TiO_2-NT-hematite modified electrode is subjected to the galvanostatic and potentiostatic polarization under pulsed light on and off conditions over time. At a constant current density of 45 μA cm^{-2}, Fig 8a, the potential under dark is ~1.1 V and after illumination as low as 0.55 V, suggesting the successful separation of the electron-hole pairs onto a modified electrode. The potential does not vary over time significantly. Under the potentiostatic conditions, Fig. 8b, at 1 V the dark current was ~45 μA cm^{-2}, while under light conditions 58 μA cm^{-2} or 27% higher. Some small deterioration of the characteristics over time is observed.

3.2. Possible application of the urea oxidation reaction

As mentioned in the Introduction, the urea could be used as good energy carriers during the water electrolysis or in the fuel cells. In Fig. 9 the structure of the potentials during anodic oxidation of 30 g dm^{-3} of urea on Pt and TiO_2-NT-hematite modified electrode, converted to electrode area of 1 m^2, as well as a polarization curve for hydrogen evolution reaction on the stainless steel electrode is shown.

The structure of the cell voltage can be given as:

$$U_{cell} = U_0 + \sum |\eta_{\pm}| + I\sum R_{\Omega} \qquad (20)$$

where U_0 is the reversible cell voltage ($U_o = E_a - E_c$), $\Sigma\eta_{\pm}$ is the sum of the absolute values of the cathodic and anodic overpotentials, and $I\Sigma R_{\Omega}$ the sum of all Ohmic drops in the cell.

The obtained open circuit voltage of the cell for hydrogen production and urea oxidation with TiO_2-NT-hematite electrode is ~0.46 V, and with platinum anode >1 V. Also, the electrolysis cell voltage, for example, at 0.4 A m^{-2} is 1.92 V for Pt anode, 1.82 V for TiO_2-NT-hematite anode under dark, or 1.47 V under light conditions, or 30% smaller energy consumption, $w = UIt$, than with the platinum anode. This analysis clearly shows that TiO_2-NT-hematite electrode possesses much smaller anodic overpotential, than Pt electrode. With further optimization, for example, using the thermally treated TiO_2-NT-hematite anode, such systems could be considered as a good catalytic materials for photo assisted electrolysis of water solutions containing urea with near neutral pH. This observation is very encouraging, because the main limit of the photo-electrochemical cells is dysfunctionality without

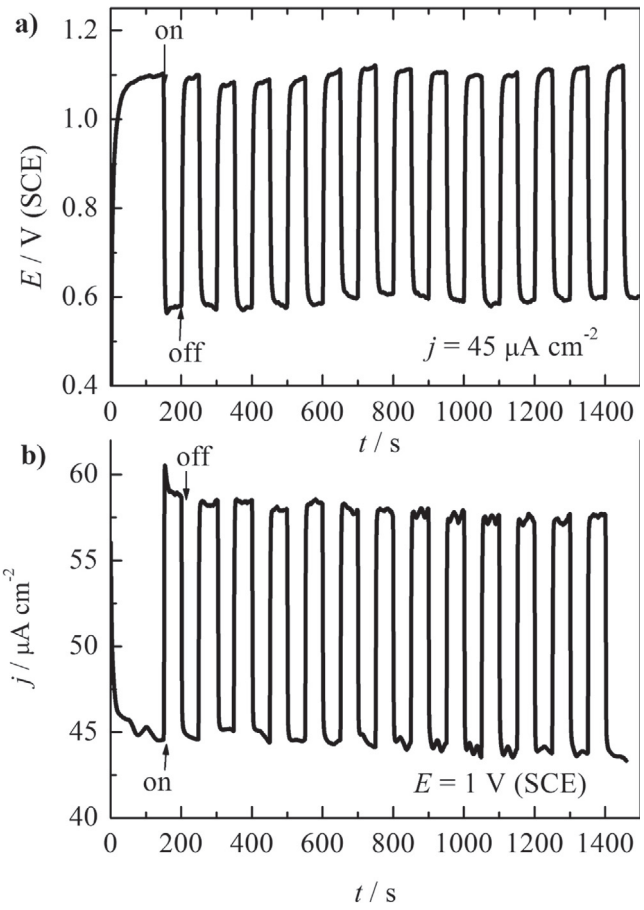

Figure 8 The galvanostatic (a) and potentiostatic (b) polarization of TiO_2-NT-hematite modified electrode (A = 2 cm^2) under pulsed light on and off conditions over time in 0.1 M Na_2SO_4 buffered with 0.05 M borax to pH = 9.2 electrolyte containing 30 g dm^{-3} urea.

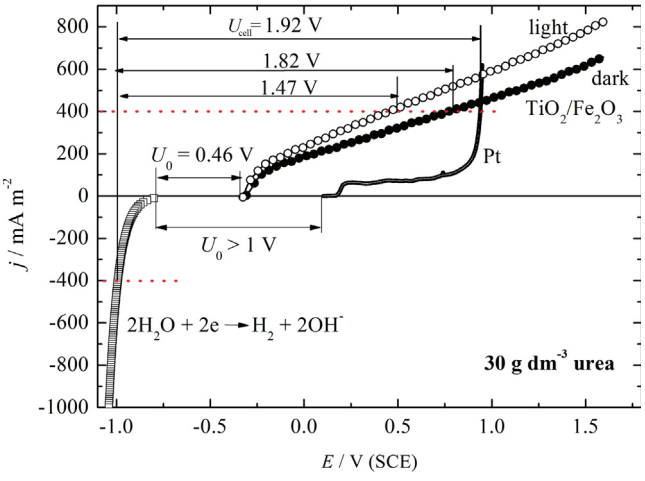

Figure 9 The structure of the cell voltage for 30 g dm^{-3} urea in the anodic oxidation on Pt (—), and TiO_2-NT-hematite electrode under dark (●) and light conditions (○), and hydrogen evolution reaction on the stainless steel electrode as cathodic reaction (□) in the 0.1 M Na_2SO_4 buffered with 0.05 M borax to pH = 9.2 electrolyte. Electrodes area are converted to 1 m^2.

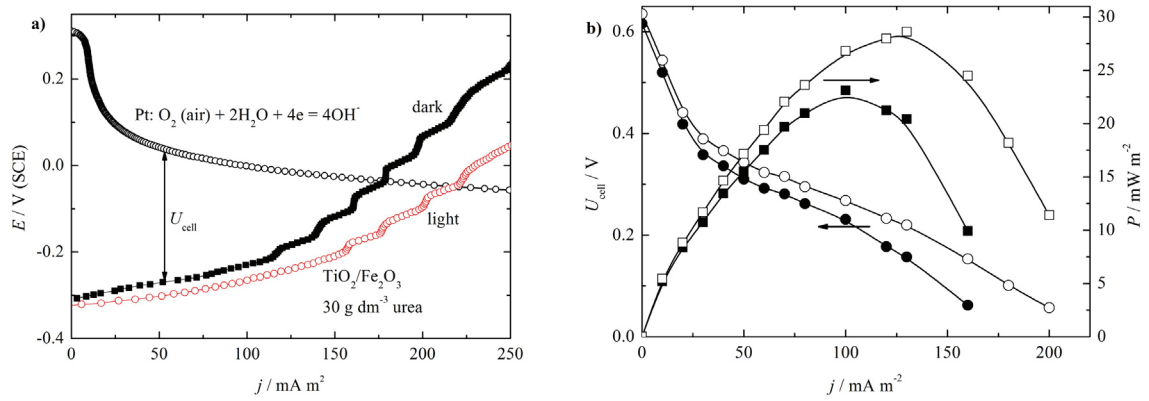

Figure 10 (a) Polarization curves of the oxygen (from air) reduction on the Pt electrode, and 30 g dm^3 urea oxidation on TiO_2-NT-hematite under dark and light conditions. (b) The dependence of the cell voltage (left), and power density (right) on current density, under dark-full symbols, and light-open symbols. (0.1 M Na_2SO_4 buffered with 0.05 M borax to pH = 9.2 electrolyte, electrodes area are converted to 1 m^2).

external light sources, which increase operational cost without Sun during the night. The TiO_2-NT-hematite anode could operate in the dark and with increased efficiency in the light conditions. Hence such a cell will not necessary require an external light source. Also, the anode can operate in the near neutral solutions, so the modification of the waste water composition by the means of increasing pH is not required.

In order to simulate possible cell voltage and the power of the fuel cell, in Fig 10a the polarization curves of the urea oxidation (under dark and light conditions) on TiO_2-NT-hematite electrode as anodic reaction, and oxygen reduction from the air on platinum as the cathodic reaction is shown. Fig. 10b shows the simulated voltage–current density curve for the possible fuel cell. It can be seen that the open circuit voltage was ~0.6 V, and operating voltage of 0.4–0.2 V is obtained for the ranges of the current density of ~25 to 150 mA m^{-2}. The maximum power density (Fig. 10b) for the fuel cell is 22 mW m^{-2} under dark and 28 mW m^{-2} under light conditions. This result also indicated that with further optimization of TiO_2-NT-hematite anode, such cell could be used for simultaneous urea degradation and electricity production, in both light and dark conditions.

4. Conclusions

It is concluded that anodically formed titanium dioxide in the shape of nanotubes modified by hematite using the successive ion layer adsorption and reaction (SILAR) method could be used as anode in the reaction of the urea oxidation. The electrode shows increased electrocatalytic activity in comparison with pure platinum anode in near neutral solutions (which are the typical conditions of the waste waters containing urea) under the dark conditions. Further improvement of the electrocatalytic behavior is observed under the electrode illumination by the light, in the so called photo assisted oxidation reaction. The possible applications of the photo assisted reaction using urea as the energy carriers are considered. It was shown that in the reaction of water electrolysis with simultaneous oxidation of urea and hydrogen production, the energy efficiency will be 30% smaller than with platinum anode. The photo-electrochemical fuel cell using oxygen reduction as a cathodic reaction is also considered with encouraging results. The open circuit voltage will be above 0.6 V, and operating cell voltage among 0.4–0.2 V. It is important to notice that both presented applications do not require modification of the electrolyte by the means of pH increase above 12, due to strong corrosion of the previously reported behavior of the anodic materials based on the nickel and cobalt.

Acknowledgement

The research was supported by the Ministry of Education, Science and Technological Development of the Republic of Serbia, under the research project "Electrochemical synthesis and characterization of nanostructured functional materials for applications in new technologies" No. ON172046. Waleed Mohammed Omymen is grateful to the Libyan Ministry of Higher Education and Scientific Research for the material supports during PhD study.

References

[1] J. Kim, D. Monllor-Satoca, W. Choi, Simultaneous production of hydrogen with the degradation of organic pollutants using TiO_2 photocatalyst modified with dual surface components, Energy Environ. Sci. 5 (2012) 7647–7656.
[2] A.N. Rollinson, J. Jones, V. Dupont, M.V. Twigg, Urea as a hydrogen carrier: A perspective on its potential for safe, sustainable and long-term energy supply, Energy Environ. Sci. 4 (2011) 1216–1224.
[3] B.K. Boggs, R.L. King, G.G. Botte, Urea electrolysis: direct hydrogen production from urine, Chem. Commun. 32 (2009) 4859–4861.
[4] P.M. Glibert, J. Harrison, C. Heil, S. Seitzinger, Escalating worldwide use of urea – A global change contributing to coastal eutrophication, Biogeochemistry 77 (3) (2006) 441–463.
[5] E. Urbańczyk, M. Sowa, W. Simka, Urea removal from aqueous solutions-a review, J. Appl. Electrochem. 46 (2016) 1011–1029.
[6] W. Yan, D. Wang, G.G. Botte, Template-assisted synthesis of Ni–Co bimetallic nanowires for urea electrocatalytic oxidation, J. Appl. Electrochem. 45 (2015) 1217–1222.
[7] P. Lianos, Production of electricity and hydrogen by photocatalytic degradation of organic wastes in a photoelectrochemical cell: The concept of the Photo fuelcell: A review of a re-emerging research field, J. Haz. Mat. 185 (2011) 575–590.

[8] R. Lan, S. Tao, J.T.S. Irvine, A direct urea fuel cell – power from fertilizer and waste, Energy Environ. Sci. 3 (2010) 438–441.
[9] W. Xu, H. Zhang, G. Li, Z. Wu, Nickel-cobalt bimetallic anode catalysts for direct urea fuel cell, Sci. Rep. 4 (2014) 5863, http://dx.doi.org/10.1038/srep05863.
[10] Â.C.S. Bezerra, E.L. de Sá, F.C. Nart, In situ vibrational study of the initial steps during urea electrochemical oxidation, J. Phys. Chem. B 101 (33) (1997) 6443–6449.
[11] J. Choulera, G.A. Padgett, P.J. Cameron, K. Preussd, M.-M. Titiricid, I. Ieropoulosf, M. Di Lorenzo, Towards effective small scale microbial fuel cells for energy generation from urine, Electrochim. Acta 192 (2016) 89–98.
[12] G. Wang, Y. Ling, X. Lu, H. Wang, F. Qian, Y. Tong, Y. Li, Solar driven hydrogen releasing from urea and human urine, Energy Environ. Sci. 5 (2012) 8215–8219.
[13] K. Cho, D. Kwonac, M.R. Hoffmann, Electrochemical treatment of human waste coupled with molecular hydrogen production, RSC Adv. 4 (2014) 4596–4608.
[14] M. Antoniadou, P. Lianos, A photoactivated fuel cell used as an apparatus that consumes organic wastes to produce electricity, Photochem. Photobiol. Sci. 10 (2011) 431–435.
[15] P. Roy, S. Berger, P. Schmuki, TiO_2 nanotubes: Synthesis and applications, Angew. Chem. Int. Ed. 50 (2011) 2904–2939.
[16] J.C. Colmenares, R. Luque, J.M. Campelo, F. Colmenares, Z. Karpiński, A.A. Romero, Nanostructured photocatalysts and their applications in the photocatalytic transformation of lignocellulosic biomass: An Overview, Materials 2 (2009) 2228–2258.
[17] Y. Lana, Y. Lub, Z. Rena, Mini review on photocatalysis of titanium dioxide nanoparticles and their solar applications, Nano Energy 2 (2013) 1031–1045.
[18] G. Cacciato, M. Zimbone, F. Ruffino, M.G. Grimaldi, TiO2 nanostructures and nanocomposites for sustainable photocatalytic water purification, Chapter 4 in: M.L. Larramendy, S. Soloneski (eds.), Green Nanotechnology – Overview and Further Prospects, InTech, 2016.
[19] X.B. Chen, S.H. Shen, L.J. Guo, S.S. Mao, Semiconductor-based photocatalytic hydrogen generation, Chem. Rev. 110 (2010) 6503–6570.
[20] Z.S. Li, W.J. Luo, M.L. Zhang, J.Y. Feng, Z.G. Zou, Photoelectrochemical cells for solar hydrogen production: current state of promising photoelectrodes, methods to improve their properties, and outlook, Energy Environ. Sci. 6 (2013) 347–370.
[21] L.Q. Jing, J. Zhou, J.R. Durrant, J. Tang, D. Liu, H. Fu, Dynamics of photogenerated charges in the phosphate modified TiO_2 and the enhanced activity for photoelectrochemical water splitting, Energy Environ. Sci. 5 (2012) 6552–6558.
[22] B. Iandolo, B. Wickman, I. Zoric, A. Hellman, The rise of hematite: origin and strategies to reduce the high onset potential for the oxygen evolution reaction, J. Mater. Chem. A 3 (2015) 16896–16912.
[23] P. Luan, M. Xie, D. Liu, X. Fu, L. Jing, Effective charge separation in the rutile TiO2 nanorod-coupled a-Fe2O3 with exceptionally high visible activities, Sci. Rep. 4 (2014) 6180, http://dx.doi.org/10.1038/srep06180.
[24] K.E. Dekrafft, C. Wang, W.B. Lin, Metal-organic framework templated synthesis of Fe_2O_3/TiO_2 nanocomposite for hydrogen production, Adv. Mater. 24 (2012) 2014–2018.
[25] W.T. Sun, Q.Q. Meng, L.Q. Jing, D.N. Liu, Y. Cao, Facile synthesis of surface-modified nanosized a-Fe_2O_3 as efficient visible photocatalysts and mechanism insight, J. Phys. Chem. C 117 (2013) 1358–1365.
[26] X. Liu, K. Chen, J.-J. Shim, J. Huang, Facile synthesis of porous Fe_2O_3 nanorods and their photocatalytic properties, J. Saudi Chem. Soc. 19 (2015) 479–484.
[27] W.M. Omymen, A.S. Ebshish, B.Z. Jugović, T. Lj, M.M. Trišović, B.N. Gvozdenović, Grgur, Photoelectochemical behavior of TiO_2-NT's modified with SILAR deposited iron oxide, Electrochim. Acta 203 (2016) 136–143.
[28] S. Bauer, S. Kleber, P. Schmuki, TiO_2 nanotubes: Tailoring the geometry in H_3PO_4/HF electrolytes, Electrochem. Commun. 8 (2006) 1321–1325.
[29] V. Cristino, S. Berardi, S. Caramori, R. Argazzi, S. Carli, L. Meda, A. Taccac, C.A. Bignozzi, Efficient solar water oxidation using photovoltaic devices functionalized with earth-abundant oxygen evolving catalysts, Phys. Chem. Chem. Phys. 15 (2013) 13083–13092.
[30] M. Žic, M. Ristić, S. Musić, Monitoring the hydrothermal precipitation of α-Fe_2O_3 from concentrated Fe(NO3)3 solutions partially neutralized with NaOH, J. Mol. Struct. 993 (2011) 115–119.
[31] W. Kraus, G. Nolze, PowderCell for Windows, V.2.4, Federal Institute for Materials Research and Testing, Berlin, Germany, 2000.
[32] B.N. Grgur, D.T. Mijin, A kinetics study of the methomyl electrochemical degradation in the chloride containing solutions, App. Cat. B: Environ. 147 (2013) 429–438.
[33] K. Siuzdak, M. Szkoda, M. Sawczaka, A. Lisowska-Oleksiak, Novel nitrogen precursors for electrochemically driven doping of titania nanotubes exhibiting enhanced photoactivity, New J. Chem. 39 (2015) 2741–2751.
[34] M. Radecka, M. Rekas, A. Trenczek-Zajac, K. Zakrzewska, Importance of the band gap energy and flat band potential for application of modified TiO_2 photoanodes in water photolysis, J. Power Sources 181 (2008) 46–55.
[35] J. Krysa, M. Zlamal, S. Kment, M. Brunclikova, Z. Hubicka, TiO_2 and Fe_2O_3 films for photoelectrochemical water splitting, Molecules 20 (2015) 1046–1058.